

A Pillared Discrete Bilayer Formed from Guanidinium and Ferrocenedisulfonate Ions: Synthesis, Crystal Structure, and Initial Electrochemical Properties

Jingli Xie,* Michelle T. Ma, Brendan F. Abrahams, and Anthony G. Wedd*

School of Chemistry and Bio21 Molecular Science and Biotechnology Institute,
The University of Melbourne, Parkville, Victoria 3052, Australia

Received June 19, 2007

The solid salt $[\text{C}(\text{NH}_2)_3]_2[\text{Fe}(\eta^5\text{-C}_5\text{H}_4\text{SO}_3)_2]$ forms a two-dimensional network based upon pillared discrete bilayers formed via charge-assisted hydrogen bonds and is electrochemically active when adhered to a glassy carbon electrode.

Charge-assisted hydrogen bonds play a significant role in crystal engineering.¹ They have been utilized to assemble coordination networks of varying dimensions, including host frameworks and even so-called nanostructures.² In particular, the use of guanidinium cations and organo-sulfonate anions (Figure 1) to optimize these intermolecular forces has allowed rational design and synthesis of a wide range of crystalline materials.^{1a,2a,3}

We are exploring ways to spontaneously assemble redox-active 2D networks on electrode surfaces, i.e., to engineer a network to bind to the electrode surface with high affinity. Substituted ferrocenes are obvious candidates as electron-transfer centers in such materials. The reaction of guanidinium chloride and ferrocene-1,1'-disulfonic acid⁴ produced the salt $[\text{C}(\text{NH}_2)_3]_2[\text{Fe}(\eta^5\text{-C}_5\text{H}_4\text{SO}_3)_2]$ (**1**) which displays a pillared discrete bilayer structure (Figure 2). This contrasts with the interdigitated monolayer structure observed in the monosulfonate salt $[\text{C}(\text{NH}_2)_3][\text{Fe}(\eta^5\text{-C}_5\text{H}_5)(\eta^5\text{-C}_5\text{H}_4\text{SO}_3)]$.⁵ Salt **1** is electrochemically active when adhered to a glassy carbon electrode.

* To whom correspondence should be addressed. E-mail: agw@unimelb.edu.au (A.G.W.), xij@unimelb.edu.au (J.X.).

- (1) (a) Ward, M. D. *Chem. Commun.* **2005**, 5838. (b) Desiraju, G. R. *Chem. Commun.* **2005**, 2995. (c) Hobza, P. *Annu. Rep. Prog. Chem., Sect. C* **2004**, 100, 3. (d) Desiraju, G. R.; Steiner, T. *The Weak Hydrogen Bond in Structural Chemistry and Biology*; Oxford University Press: Oxford, 1999. (e) Beatty, A. M. *CrystEngComm* **2001**, 1, 1. (f) Sherrington, D. C.; Taskinen, K. A. *Chem. Soc. Rev.* **2001**, 30, 83. (g) Desiraju, G. R. *Angew. Chem., Int. Ed. Engl.* **1995**, 34, 2311.
- (2) (a) Holman, K. T.; Pivovar, A. M.; Swift, J. A.; Ward, M. D. *Acc. Chem. Res.* **2001**, 34, 107. (b) Russell, V. A.; Ward, M. D. *Chem. Mater.* **1996**, 8, 1654. (c) Beatty, A. M. *Coord. Chem. Rev.* **2003**, 246, 131.
- (3) (a) Russell, V. A.; Evans, C. C.; Li, W.; Ward, M. D. *Science* **1997**, 276, 575. (b) Custelcean, R.; Ward, M. D. *Cryst. Growth Des.* **2005**, 5, 2277.

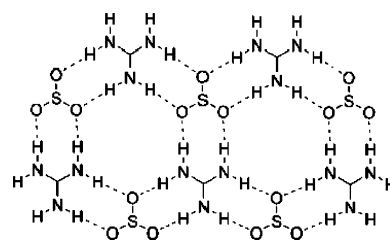


Figure 1. Quasi-hexagonal (6,3) net formed by guanidinium and sulfonate ions. Each ion is involved in six charge-assisted N–H···O hydrogen bonds.

Crystal structure analysis⁶ revealed that **1** crystallized in the triclinic $P\bar{1}$ space group with one crystallographically independent guanidinium ion in the asymmetric unit (Figure 2a). The iron atom Fe(1) occupied a center of symmetry and the ferrocene unit adopted a staggered configuration. All Fe–C bond lengths [1.992(8)–2.056(8) Å] are within the

- (4) Preparation of salt **1**. Ferrocenedisulfonic acid (0.346 g; 1 mmol) was dissolved in DMF (10 ml). Guanidinium chloride (0.191 g; 2 mmol) was added, and the solution stirred at room temperature for 10 min. After filtration, diethyl ether was allowed to diffuse into the solution providing yellow needlelike X-ray quality single crystals in 1 week. Yield, 0.376 g (81 %). Anal. Calcd (%) for $\text{C}_{12}\text{H}_{20}\text{FeN}_6\text{O}_6\text{S}_2$: C 31.04, H 4.34, N 18.10, O 20.68, S 13.81. Found C 30.98, H 4.39, N 18.20, O 20.74, S 13.84. (Chemical & MicroAnalytical Services Pty. Ltd., Belmont, VIC, Australia). ¹H NMR (500 MHz, $(\text{CD}_3)_2\text{SO}$, 25 °C): δ 4.1 (s, C_5H_4 , 4H), 4.3 (s, C_5H_4 , 4H), 6.95 (s, $\text{C}(\text{NH}_2)_3$, 12H), (Figure S1). FTIR data ($\nu_{\text{max}}/\text{cm}^{-1}$): 3328(s), 3183(s), 2818(w), 1674(s), 1581(m), 1176(s), 1058(s), 1043(s), 1013(s), 891(w), 824(s), 743(m), (Figure S2). ESI-MS (cone voltage, 80 V; m/z range, 0–800): positive ion, m/z 60.0, $[\text{C}(\text{NH}_2)_3]^+$; negative ion, m/z 172.0 = 344/2, $[\text{Fe}(\eta^5\text{-C}_5\text{H}_4\text{SO}_3)_2]^{2-}$.
- (5) Russell, V. A.; Ward, M. D. *J. Mater. Chem.* **1997**, 7, 1123.
- (6) Crystal data for **1**: $\text{C}_{12}\text{H}_{20}\text{FeN}_6\text{O}_6\text{S}_2$, $M = 464.31$, triclinic, space group $P\bar{1}$, $a = 7.156(5)$ Å, $b = 7.268(5)$ Å, $c = 11.408(7)$ Å, $\alpha = 99.314(14)^\circ$, $\beta = 98.722(15)^\circ$, $\gamma = 119.088(12)^\circ$, $V = 493.1(5)$ Å³, $Z = 1$, $D_c = 1.564$ g cm⁻³, $\lambda = 0.71073$ Å. Data on a crystal of dimensions $0.22 \times 0.08 \times 0.05$ mm³ were collected at 293 K. GOF = 1.007. Total of 2132 reflections (1297 unique) with $R_{\text{int}} = 0.0916$, $R_1 = 0.0889$ ($I > 2\sigma(I)$), $wR_2 = 0.2660$ (all data). CCDC 620270. The structure of **1** was solved using direct methods (SHELXL V5.1)⁷ from single-crystal data on a Bruker SMART/CCD area detector diffractometer fitted with Mo K_α radiation ($\lambda = 0.71073$ Å) and a graphite monochromator. Structure refinements were performed using the SHELXL97 program, which uses a full-matrix least-squares refinement based on F^2 .⁷ All non-hydrogen atoms except the carbon atoms on ferrocene rings were refined with anisotropic thermal displacement parameters.

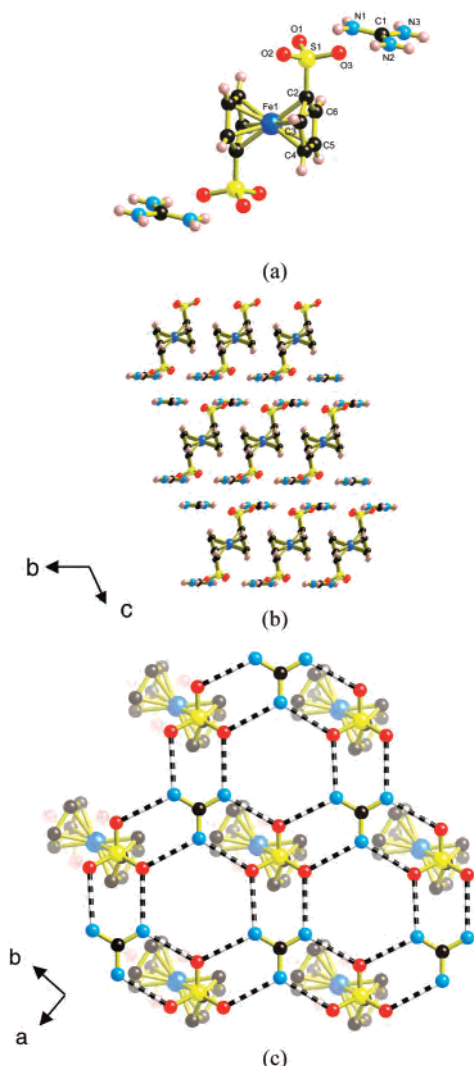


Figure 2. (a) Molecular structure of **1**. (b) 2D network structure of **1** (pillared discrete bilayer) when viewed along the *a* axis. (c) Quasi-hexagonal (6,3) net formed by guanidinium and ferrocenedisulfonate ions when viewed along the *c* axis.

ranges observed in related complexes.⁵ Charge-assisted hydrogen bonding between the ions enforced the quasi-hexagonal (6,3) net (Figure 1) within a lamellar architecture with six charge-assisted N–H···O hydrogen bonds per guanidinium ion (Table S1). The staggered configuration of the ferrocene unit leads to a well-defined pillared discrete bilayer (Figure 2b), as seen in other organodisulfonate networks.^{1a,2a} If based on the nearest S···C distance, the interlamellar space is around 3.95 Å.

Ferrocenemonosulfonate derivatives have been explored as electron mediators in redox enzyme catalysis and in doped polyaniline electrodes.⁸ Here we report initial results on immobilization of the bilayer ferrocenedisulfonate salt **1** on a glassy carbon working electrode.⁹

Salt **1** is soluble in water and *N,N'*-dimethylformamide (DMF) but insoluble in MeCN. It exhibited a reversible,

(7) Sheldrick, G. M. *SHELXS-97, Programs for the solution of crystal structures*; Institut für Anorganische Chemie der Universität: Göttingen, Germany, 1997. Sheldrick, G. M. *SHELXL-97, Programs for the refinement of crystal structures*; Institut für Anorganische Chemie der Universität: Göttingen, Germany, 1997.

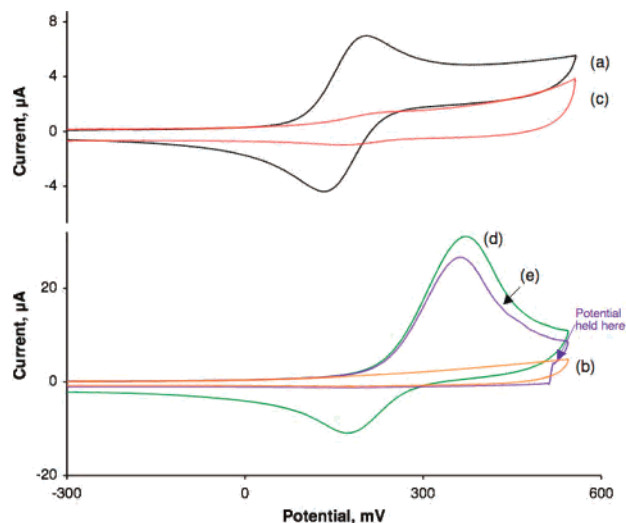


Figure 3. Cyclic voltammetry of **1** (ν , 100 mV s^{-1}): (a) black, saturated solution in $\text{H}_2\text{O}/\text{MeCN}$ (7.5:92.5 v/v; Bu_4NBF_4 , 0.05 M); (b) orange, saturated solution in $\text{H}_2\text{O}/\text{MeCN}$ (7.5:92.5 v/v; $[\text{C}(\text{NH}_2)_3]\text{Cl}$, 0.05 M); (c) red, saturated solution in $\text{H}_2\text{O}/\text{MeCN}$ (10.0:90.0 v/v; $[\text{C}(\text{NH}_2)_3]\text{Cl}$, 0.05 M); (d) green, powdered sample attached mechanically to the polished glassy carbon electrode in contact with a saturated solution in $\text{H}_2\text{O}/\text{MeCN}$ (7.5:92.5 v/v; $[\text{C}(\text{NH}_2)_3]\text{Cl}$, 0.05 M); and (e) purple, same as (d) but the potential was held for 30 s at the anodic limit.

diffusion-controlled, one-electron event (Figure 3a) in the electrolyte $\text{H}_2\text{O}/\text{MeCN}$ (7.5:92.5 v/v; Bu_4NBF_4 , 0.05 M), typical of ferrocene derivatives. For cyclic voltametric scan rates, ν , in the range 20–1000 mV s^{-1} , $I_p^{\text{ox}}/I_p^{\text{red}}$ was close to unity and ΔE_p was 75 mV for a scan rate of 100 mV s^{-1} , indistinguishable from that obtained for the ferrocene reference standard under the same conditions. The difference from the theoretically predicted value of 56 mV at 20 °C can be attributed to a low level of uncompensated resistance.¹⁰ Change of the supporting electrolyte from Bu_4NBF_4 (0.05 M) to $[\text{C}(\text{NH}_2)_3]\text{Cl}$ (0.05 M) reduced the solubility of **1** (via the common ion effect), and no current response was detectable (Figure 3b). However, an increase of the proportion of water from 7.5 to 10 vol % in the electrolyte $\text{H}_2\text{O}/\text{MeCN}$ (10.0:90.0 v/v; $[\text{C}(\text{NH}_2)_3]\text{Cl}$, 0.05 M) increased the solubility of **1** sufficiently to allow observation of the reversible response of a saturated solution of **1** in this electrolyte (ν , 100 mV s^{-1} ; Figure 3c). The change of electrolyte shifted the reversible potential $E^{0'}$ = $(E_p^{\text{red}} + E_p^{\text{ox}})/2$ from 163 to 187 mV (vs Fc^+/Fc), presumably due to the effects of charge-assisted hydrogen bonding between the sulfonate and guanidinium centers.

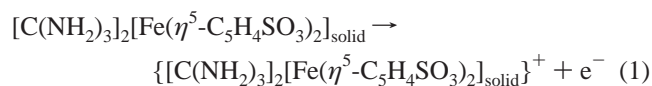
(8) (a) Liaudet, E.; Battaglini, F.; Calvo, E. J. *J. Electroanal. Chem.* **1990**, 293, 55. (b) Ryabov, A. D.; Goral, V. N. *J. Biol. Inorg. Chem.* **1997**, 2, 182. (c) Shan, D.; Mu, S. *Synth. Met.* **2002**, 126, 225.

(9) Voltametric experiments were performed with an Autolab (Eco Chemie, Utrecht, Netherlands) computer-controlled electrochemical workstation. Media were CH_3CN and $\text{CH}_3\text{CN}/\text{H}_2\text{O}$ mixtures with 0.05 M $\text{Bu}_4\text{N}^+\text{BF}_4^-$ or $[\text{C}(\text{NH}_2)_3]\text{Cl}$ as supporting electrolyte (see caption of Figure 3 for details). A standard three-electrode arrangement was used with a glassy carbon disk (d, 3 mm) as working electrode, a Pt wire as auxiliary electrode and a Ag/Ag^+ reference electrode (silver wire in MeCN (Bu_4NBF_4 (0.1 M) AgNO_3 (0.01 M)). Scan rate: 100 mV s^{-1} , sample interval: 0.45 mV, sensitivity: 1×10^{-4} A V^{-1} . All quoted potentials are referenced to the Fc^+/Fc couple.

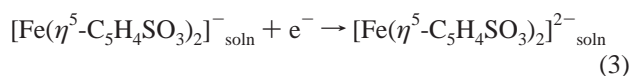
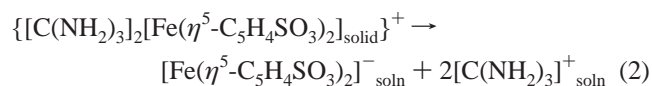
(10) Bard, A. J.; Faulkner, L. R. *Electrochemical methods: fundamentals and applications*, 2nd ed.; Wiley: New York, 2001.

The procedure for mechanical attachment of microcrystalline solids onto electrode surfaces has been described in detail previously.¹¹ In brief, powdered **1** was attached mechanically to the polished surface of the working electrode via a cotton bud. The electrode was then placed in contact with the electrolyte solution used to obtain Figure 3b (saturated solution of **1** in H₂O/MeCN (7.5:92.5 v/v; [C(NH₂)₃]Cl, 0.05 M)).

The change in electrochemical response was dramatic: the oxidative current observed increased by a factor of at least 50 relative to that observed at the unmodified electrode in contact with the same electrolyte (compare curves b and d of Figure 3; ν , 100 mV s⁻¹). The response at E_p^{ox} , 375 mV in Figure 3d is attributed to oxidation of surface-confined **1** (eq 1):¹²



Reversal of the scan led to detection of a reduction response at E_p^{red} , 170 mV. The shape of the peak is typical of a diffusion-controlled process for reduction of one-electron oxidized **1** in solution, and E_p^{red} is close to that observed for solutions of **1** (compare curve d with curves a and c of Figure 3). This process is attributed to reduction of oxidized **1** in solution following rapid dissolution of the oxidized solid from the electrode surface (eqs 2, 3):



This interpretation is supported by the experiment shown in Figure 3e where the oxidative scan was held at the potential of the anodic limit for 30 s. The return scan showed no reductive component, consistent with oxidation of all surface-confined **1** and diffusion of the oxidized anion away from the electrode on the time scale of the experiment. The interpretation is supported by related experiments at ν , 100 and 1000 mV s⁻¹: multiple scans lead to loss of electroactive material (Figure S3).

In summary, these experiments demonstrate that the discrete bilayer salt **1** is electrochemically active in the solid state. Further investigation of its redox properties and those of derivatives are being pursued. The aim is to produce modified materials in which a single discrete bilayer (such as that present in salt **1** (Figure 2b)) spontaneously assembles as a redox-active 2D network on electrode surfaces. This requires sufficient affinity for those surfaces to prevent the dissociation observed for oxidized **1** (eq 2) which, in turn, requires differentiation of the two surfaces of the bilayer.

Acknowledgment. The authors are grateful to financial support by the Australian Research Council under Grants No. DP0770585 (J.X.) and DP0450134 (A.G.W.).

Supporting Information Available: Crystallographic data in CIF format, hydrogen-bonding parameters, ¹H NMR and IR spectroscopy of **1**, and multiple-scan cyclic voltammetry of surface-confined salt **1** under the conditions of Figure 3d. This material is available free of charge via the Internet at <http://pubs.acs.org>.

IC7011974

- (11) Bond, A. M.; McLennan, E. A.; Stojanovic, R. S.; Thomas, F. G. *Anal. Chem.* **1987**, *59*, 2853.
- (12) The oxidative wave shape of Figure 3d is consistent with the symmetric shape expected for a surface-confined process. Deviation from that shape at high potentials is consistent with the background contribution from the diffusion-controlled oxidation of **1** in this saturated solution (Figure 3b).